Indian J Phys
https://doi.org/10.1007/s12648-024-03332-y

ORIGINAL PAPER

Study of relativistic charged particle production using multi-source thermal model and emission feature of slowest target protons

K Attri[1], M K Singh[1]* and P K Khandai[2]

[1]Department of Physics, Institute of Applied Sciences and Humanities, GLA University, Mathura 281406, India

[2]Department of Physics, Ewing Christian College, Allahabad 211003, India

Received: 23 April 2024 / Accepted: 26 June 2024

Abstract: In this manuscript we have mainly focused our study on the multiplicity distributions of projectile fragments and slowest target protons (black particles) released during the interaction of ^{84}Kr with emulsion at 1 A GeV and their dependency on various target groups of the nuclear emulsion. In case of projectile fragments these distributions are described and have been replicated using a multi-source thermal model. The model makes the premise that collisions produce a large number of particle sources. Like a radioactive item, each source contributes a multiplicity distribution. The observations of the present study shows that the theoretical calculations utilising the multi-source thermal model and the experimental findings are in good agreement. In case of slowest target protons this study reveals a striking relationship between the target fragmentation processes and collision geometry with multiplicity distributions.

Keywords: RHIC; Emulsion technology; Multi-source thermal model; Slowest target protons

1. Introduction

Following the prediction of the QGP as a new phase of matter, physicists worldwide focused much attention on the nucleus-nucleus (A-A) and hadron-nucleus (h-A) interactions because they offer concise information on properties of nuclear matter, such as quarks, gluons, and nuclear matter density [1–6]. High spatial resolution nuclear emulsion detector (NED) enable the detection of short-lived particles like charm mesons and other similar particles [7–9].

The three zones of the interacting systems are based on the Participant Spectator (PS) model [10, 11]. Figure 1 displays the PS model schematic diagram. The projectile spectator region comes first. The projectile's velocity and the velocity of the projectile spectator zones are virtually equal. Projectile fragments are the particles created from the projectile spectator areas and have a charge of $Z \geq 1$. The intended spectator zone comes in second. In the frame of reference of the laboratory, the velocity of the target spectator zone is zero. Target fragments are the byproducts of the target spectator areas. Target and projectile spectator zones are not interacting with each other. The third is the participant region, which is the area where the projectile and the target nuclei intersect. The participant region emits the newly created particles (like pions, kaons, mesons, etc.) [10, 11].

Friction is thought to be created on the contact layer in collisions due to the existence of relative motion between the participant and the spectator. Due to friction, both the participant and the spectators get heated in this condition. As depicted in Fig. 1, the contact layer and the remainder section, which are separated by heat of friction, are thought to represent two sources of nuclear fragments with distinct temperatures. This might cause the entire target spectator to enter a non-equilibrium state, yet the contact layer and the remainder of the spectator to remain in a local equilibrium condition [10]. Grey particles, also referred to as fast target protons, are released from the target spectator's contact layer, while black particles, also known as slow target protons, are released from the target spectator's rest part [10].

Numerous research works have been done on multiplicity, including theoretical and experimental ones. Understanding the multiplicity of secondary charged particles is essential to comprehending the process of nucleus-nucleus interactions, since it is one of the most important

*Corresponding author, E-mail: singhmanoj59@gmail.com

Published online: 10 July 2024

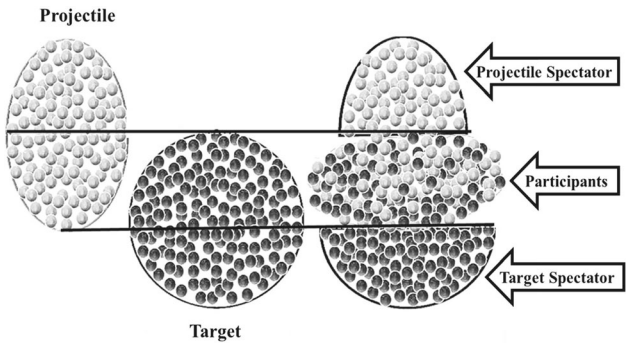

Fig. 1 An illustration of the PS model [11]

and easily measured factors defining any heavy-ion collisions at high energies [12, 13]. Important details can be uncovered by comparing the average multiplicity and its distributions with the theoretical predictions of different computations.

In this work, we have primarily examined the multiplicity distributions of the projectile fragments (PFs) released during ^{84}Kr emulsion interactions at 1 A GeV and their dependence on different emulsion target groups. Using a multi-source thermal methodology, these distributions are characterized and verified. Additionally, we looked at the black particle multiplicity distribution and how it was impacted by the interactions between the various target nuclei in the nuclear emulsion.

2. Experimental details

Germany's Gesellschaft *fr* Schwerionenforschung (GSI) Darmstadt created a NED. Projectiles consisting of ^{84}Kr nuclei with incidence kinetic energy of 1 GeV per nucleon and 98–95% of ^{84}Kr with 2–5% impurities were used in the experiment [8–13]. The investigation used NED with a size of $9.8 \times 9.8 \times 0.06$ cm^3 [14–16]. Figure 2 displays the photo of the NED. The Olympus BH-2 binocular microscope was utilized to scan the event of interest. The binocular microscope's primary parts include many dry and oil immersion objectives with magnifications of 10X, 20X, 40X, 60X, and 100X. The air between the NED and lense was removed using sandal wood oil while utilizing a 100X objective.

Fig. 2 An illustration of the NED [11]

In the present study, an Olympus BH-2 binocular microscope was utilized to scan the event of interest from the NED utilizing the two most popular scanning techniques: line scanning and volume scanning. Tracking the events is necessary for line scanning until they interact or depart off the NED. Having scanned the events strip by strip during volume scanning, we will be able to scan low energy events using this scanning technique. After detecting the events through volume scanning, we follow the event tracks to ascertain their velocity. As background events might interact anyplace on the NED, we must pay close attention to what is going on there. They have, however, vanished, leaving no discernible mark on the NED, as we discover when we return to look for their tail [11–15]. We used every effort to confirm that the projectile engagements with the emulsion target were the source of the occurrences, hence confirming their authenticity. Due to the manual, non-automatic nature of the scanning process and the age of the NED, we have added 2% of systematic error in our study. These two scanning techniques have yielded 700 occurrences, which will be subjected to a more thorough physics study. The events scanning was carried out at the BHU, Varanasi, India. Important events are compiled, and based on their features, they are categorized into different groupings. Target fragments are classified into three main types based on their relative range (L) on the NED, relative velocity (β), and normalised grain density (g^*) [14–18]. *2.1. Grey particles*; It is represented by N_g and has $L > 3$ mm, $0.3 \leq \beta < 0.7$, and $1.4 < g^* < 6.8$. It is also known as fast target proton [16]. *2.2. Black particles*; It is represented by N_b and has $L \leq 3$ mm, $g^* \geq 6.8$, and $\beta < 0.3$. It is also known as slow target proton [14, 16]. *2.3. Shower particles*; It is represented by N_s and has $\beta \geq 0.7$ and $g^* \leq 1.4$ [14, 18]. Heavily ionizing charged particles (N_h) indicates the total number of black and grey particles [14–18].

3. The multi-source thermal model

The multi-source thermal model, which is mostly employed in the descriptions of transverse flows in A-A collisions, particle emission angles and azimuthal angles serves as the foundation for the physics picture of the present analysis [19–21]. The fundamental presumption of

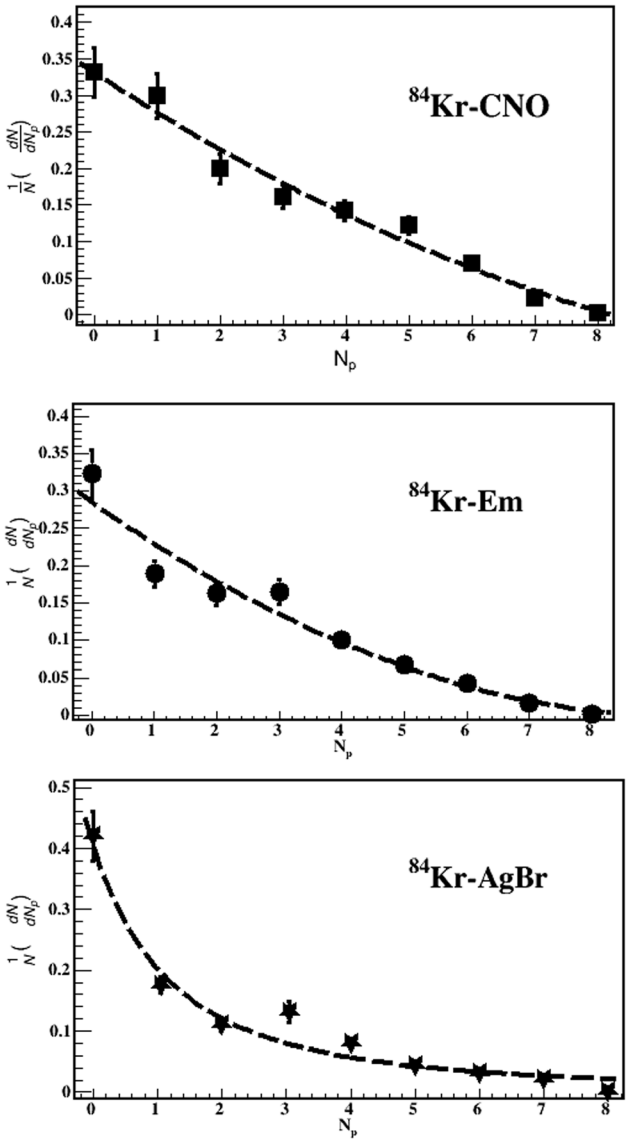

Fig. 3 The N_p normalized multiplicity distributions in the interaction of the ^{84}Kr projectile with (up) CNO, (mid) Em and (bottom) AgBr targets respectively. The curves indicate the theoretical findings using the model

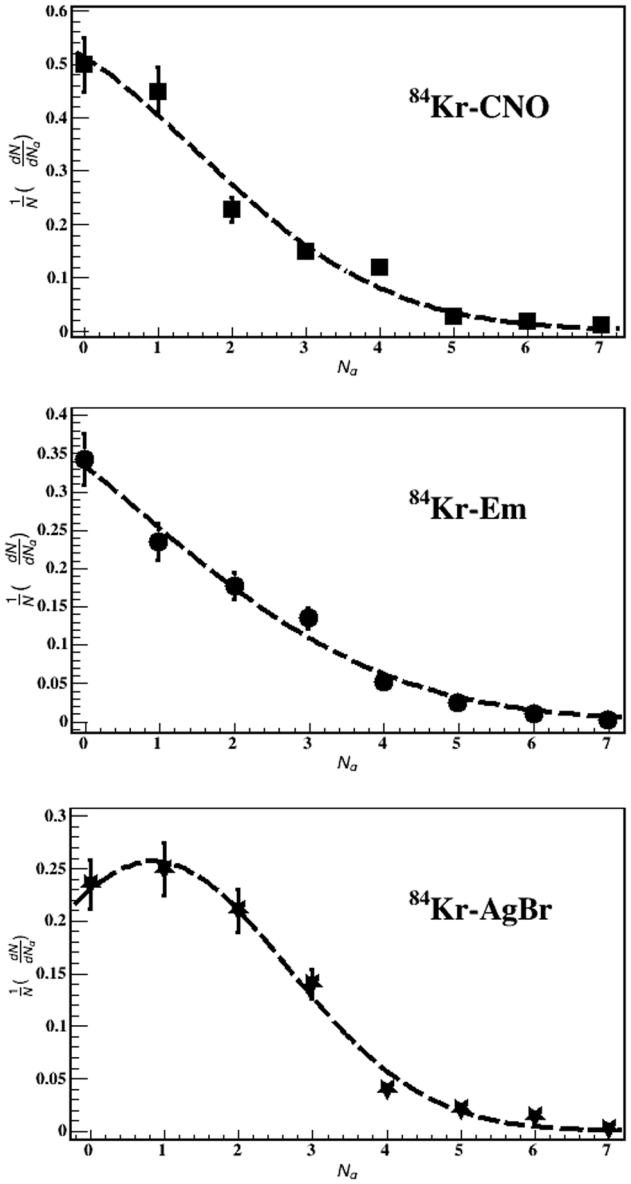

Fig. 4 The N_α normalized multiplicity distributions in the interaction of the ^{84}Kr projectile with (up) CNO, (mid) Em and (bottom) AgBr targets respectively. The curves indicate the theoretical findings using the model

the model is that many sources of producing particles and fragments are assumed to form in high-energy collisions [19–21]. Based on this model the experimental event sample has been separated into l groups (sub-samples) based on impact parameters and reaction mechanisms including evaporation, absorption, spallation, multi-fragmentation etc [19–21]. The multi-source thermal model generates a multi-component Erlang distribution in the multiplicity distribution that describes many types of particles as well as fragments [20–22]. Let's assume that the jth group has β_j sources. The multiplicity distribution is expected to take an exponential from each source. As a result, the multiplicity α_{ij} distribution that the ith source in the jth group provided is as follows:

$$P_{ij}(\alpha_{ij}) = \frac{1}{<\alpha_{ij}>} exp\left(-\frac{\alpha_{ij}}{<\alpha_{ij}>}\right) \quad (1)$$

where the ith source in the jth group contributes to $<\alpha_{ij}>$, the mean multiplicity, which is unrelated to i. The jth group contributed a multiplicity distribution that is an Erlang distribution [23].

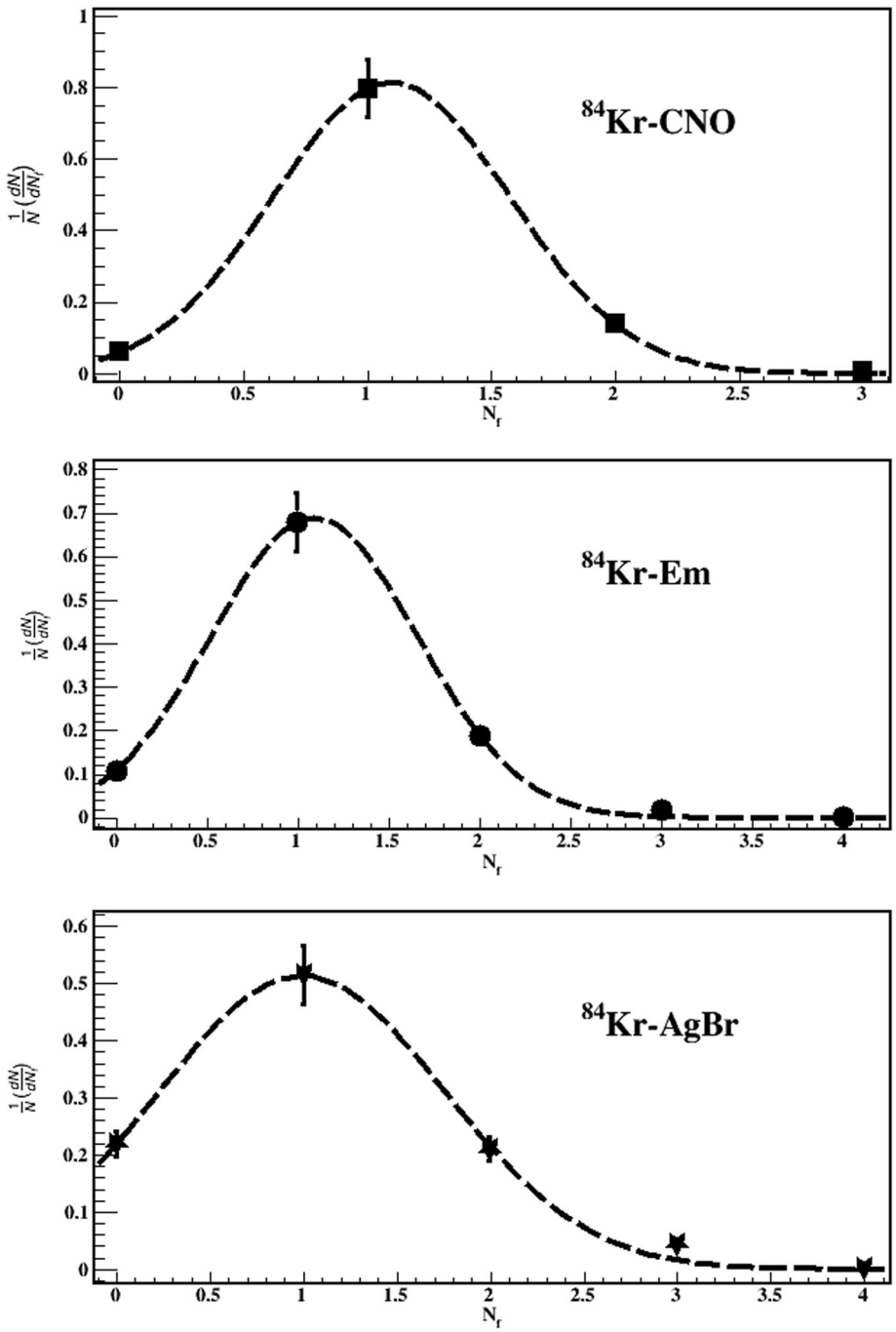

Fig. 5 The N_f normalized multiplicity distributions in the interaction of the ^{84}Kr projectile with (up) CNO, (mid) Em and (bottom) AgBr targets respectively. The curves indicate the theoretical findings using the model

$$P_j(\alpha_x) = \frac{\alpha_x^{\beta_j - 1}}{(\beta_j - 1)! < \alpha_{ij} >} exp\left(-\frac{\alpha_x}{< \alpha_{ij} >}\right) \quad (2)$$

It is the folding result of β_j exponential functions and $\alpha_x = \Sigma_{i=1}^{\beta_j} \alpha_{ij}$ and x denotes N_p, N_α, and N_f respectively. The sum of the l group contributions is weighted to create the final multiplicity distribution. Then we have,

$$P(\alpha_x) = \frac{1}{N}\frac{dN}{d\alpha_x} = \Sigma_{j=1}^{l} k_i P_j(\alpha_x) \quad (3)$$

where k_i and N stand for the weight factor and the number of particle fragments, respectively. The weight factor k_i is obtained by the geometrical weight of the impact parameter [20, 21]. In the present analysis the value of k_i is taken as 1.

Let R_{ij} stand for random numbers between 0 and 1 when using the Monte Carlo method. Then Eqs. (1) and (2) result in,

$$\alpha_{ij} = - < \alpha_{ij} > lnR_{ij} \quad (4)$$

and

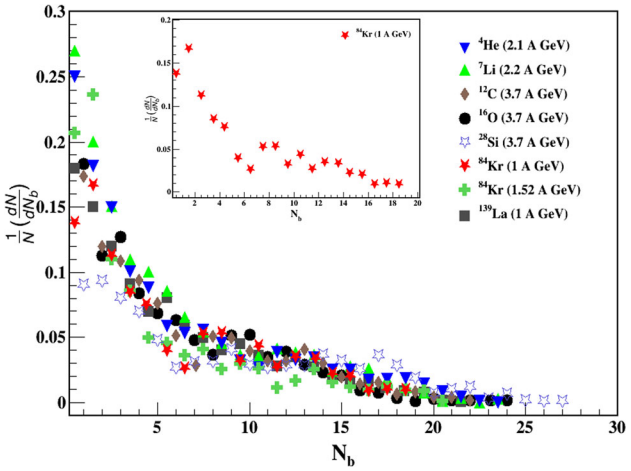

Fig. 6 The N_b normalized multiplicity distributions in the interaction of ^{4}He [29], ^{7}Li [29], ^{12}C [28], ^{16}O [28], ^{28}Si [30], ^{84}Kr [present work], ^{84}Kr [29], ^{139}La [29] with emulsion

$$\alpha_x = -\Sigma_{i=1}^{\beta_j} < \alpha_{ij} > lnR_{ij} \tag{5}$$

Finally, a statistical method is used to determine the multiplicity distribution in accordance with various k_j [24, 25]. The mean multiplicities that the jth group and the l groups contributed are given by,

$$< \alpha_x > \; = \beta_j < \alpha_{ij} > \tag{6}$$

and,

$$< \alpha_x > \; = \Sigma_{j=1}^{l} k_j \beta_j < \alpha_{ij} > \tag{7}$$

4. Results and discussion

We have classified the NED nuclei into three groups, AgBr, H and CNO in order to examine the multiplicity behavior of emerged fragments. This is because we are aware that the NED is a mixed target detector. The N_h value for AgBr is more than 8 and less or equal to 1 for H. While for CNO it is in the range of 2–8 [26].

The PFs having charge $Z \geq 1$ are divided into three main categories. First of them is called singly-charged PFs (N_p) having charge 1. Second is doubly-charged PFs (N_α) which have double charge. And third is multiple-charged PFs (N_f) having charge more than two [24].

The normalised multiplicity distributions of the PFs N_p, N_α, and N_f in ^{84}Kr contacts with various target groups of emulsion at 1 A GeV are shown in Figs. 3, 4 and 5. The curves indicate the theoretical findings using the multi-source thermal model, whereas the data points represent observed experimental data. In every instance, the computed results and the observed experimental data correspond fairly well.

The singly charged PFs, multiplicity distribution with different emulsion targets is shown in Fig. 3. It can be noticed, from all these figures, that the emission probability

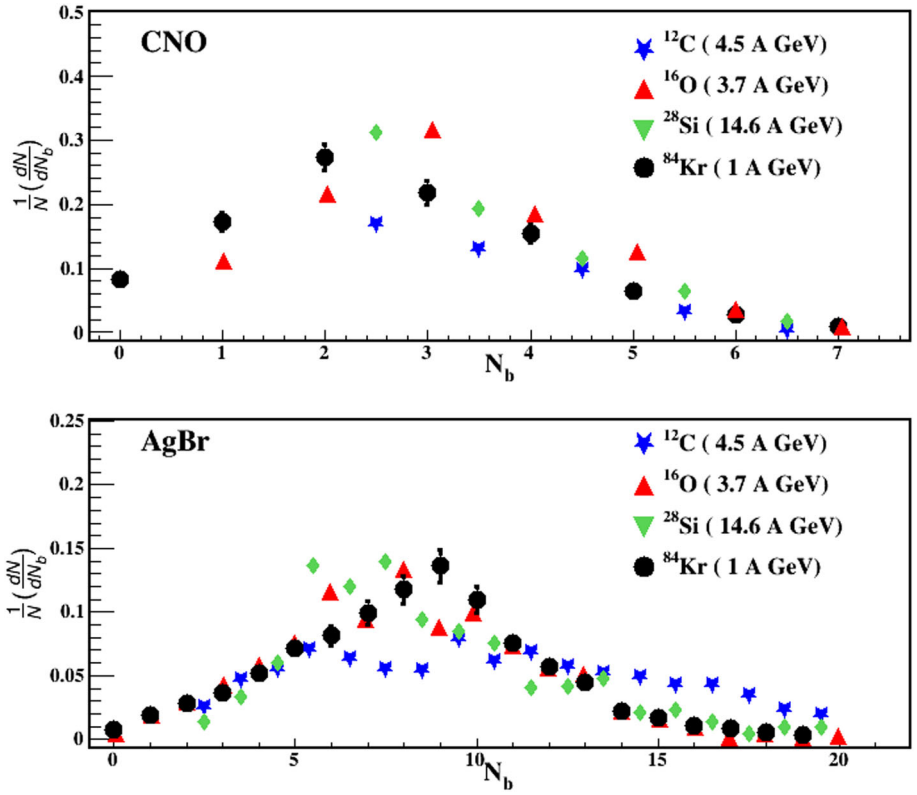

Fig. 7 The N_b normalized multiplicity distributions in the interaction of ^{12}C [31], ^{16}O [28], ^{28}Si [31], ^{84}Kr [present work] with (up) CNO (down) AgBr target of NED

of single charge PFs decreases as we move lower to higher numbers and this decreasing behaviour is changing sharply as we move from light nuclei to heavy nuclei. As a result, protons become less numerous as target nuclei's mass increases.

Figure 4 shows the multiplicity distribution of doubly charged PFs with different emulsion targets. From Fig. 4 we can see that these distributions have the same trend as in Fig. 3 for light nuclei, intermediate nuclei and Em, while in case of heavy nuclei it is little bit difference, this behaviour show that the higher number of doubly charged PFs emitted within this interaction. Such type of behaviours in case of doubly charged PFs are also observed by other experimental observations [19, 27].

Figure 5 shows the multiplicity distribution of multiple charged PFs with different emulsion targets. From Fig. 5 we can see in every time, there is a reasonable correlation between the computed results and the experimental data collected.

Figure 6 shows the comparison between the normalized multiplicity distributions of N_b produced in the interaction of the projectiles ^{4}He (2.1 A GeV), ^{7}Li (2.2 A GeV), ^{12}C (3.7 A GeV), ^{16}O (3.7 A GeV), ^{28}Si (3.7 A GeV), ^{84}Kr (1 A GeV), ^{84}Kr (1.52 A GeV), ^{139}La (1 A GeV) with emulsion. The normalized data presented in Fig. 6 show a similar pattern in N_b production, indicating that the emission of these particles is likely to be caused by a single isotropic process. These particles emit isotropically, regardless of projectile mass, by an evaporation process from the thermalized target nucleus.

Figure 7 shows the comparison between the normalized multiplicity distributions of N_b produced in the interaction of the projectiles ^{12}C (4.5 A GeV), ^{16}O (3.7 A GeV), ^{28}Si (14.6 A GeV), ^{84}Kr [present work] with CNO and AgBr target of NED. From Fig. 7 it is clear that the emission rate of N_b particles is higher with AgBr-target interaction as compared to CNO-target interaction for different projectiles having various incident kinetic energy, which demonstrate that the emission of N_b not depending on the projectile mass while strongly depending on the target mass.

5. Conclusions

When ^{84}Kr interacts with an emulsion at 1 A GeV, several target nuclei's constituent parts are studied to determine the multiplicity properties of the PFs released. These findings have been contrasted with the current computations, which are based on a multi-source thermal model. According to this study, the multi-source thermal model and the observed experimental data show a reasonable amount of consistency. The typical multiplicities of PFs for a given projectile depend on the target mass.

Moreover, the fact that the N_b particle emission in projectile impacts at different energies is identical indicates that a single isotropic process is responsible for the emission of these particles. Regardless of their projectile mass number, the isotropic emission of these particles is identified as an evaporation process from the thermalized target nucleus.

Acknowledgements Thank you to the technical team at GSI in Germany for exposing the NED with ^{84}Kr at 1 A GeV.

References

[1] J Boguta *Phys. Lett. B* **109** 251 (1982)
[2] S Ahmad et al *Inter. J. Mod. Phys. E* **18** 1929 (2009)
[3] H Stocker *Nucl. Phys. A* **750** 121 (2005)
[4] S Ahmad et al *Nature* **403** 581 (2000)
[5] M K Singh et al *Indian J. Phys.* **88** 323 (2014)
[6] D Teaney et al Phys. Rev. Lett. **86** (2001)
[7] M K Singh et al *Indian J. Phys.* **84** 1257 (2010)
[8] M K Singh et al Chinese *J. Phys.* **67** 107 (2020)
[9] U Singh et al *J. Kor. Phys. Soc.* **76** 297 (2020)
[10] M K Singh et al *Indian J. Phys.* **85** 1523 (2011)
[11] M K Singh et al *Eur. Phys. J. Plus* **135** 740 (2020)
[12] U Singh et al *Indian J. Pure & Applied Phys.* **58** 368 (2020)
[13] S Kumar et al *Int. J. Mod. Phys. E* **29** 2050077 (2020)
[14] M K Singh et al *Eur. Phys. J. Plus* **136** 419 (2021)
[15] B Kumari et al *Int. J. Mod. Phys. E* **31** 2250061 (2022)
[16] S Kumar et al *Eur. Phys. J. Plus* **136** 115 (2021)
[17] Kajal et al *Int. J. Mod. Phys. E* **31** 2250073 (2022)
[18] S Bhattacharyya *Eur. Phys. J. A* **57** 164 (2021)
[19] F H Liu *Chin. J. Phys.* **41** 486 (2003)
[20] F H Liu et al *Phys. Rev. C* **78** 044602 (2008)
[21] F H Liu *Nucl. Phys. A* **810** 159 (2008)
[22] Y Q Gao et al Pramana *J. Phys.* **79** 1407 (2012)
[23] U Rawat et al *J. Kor. Phys. Soc.* **83** 411 (2023)
[24] F H Liu *Phys. Let. B* **583** 68 (2004)
[25] F H Liu et al *Phys. Rev. C* **69** 057601 (2004)
[26] N Marimuthu et al *Int. J. Mod. Phys. E* **328** 1950098 (2019)
[27] M A Rahim *Eur. Phys. J. A* **48** 115 (2012)
[28] S Kamel et al *Int. J. Mod. Phys. E* **30** 2150042 (2021)
[29] B Kumari et al *J. Phys. Soc. Jpn.* **92** 124203 (2023)
[30] A Kumar et al Pramana *J. Phys.* **84** 591 (2015)
[31] M A Ahmad et al *Int. J. Theo. Appl. Phys.* **2** 199 (2012)